IAI
Journals.ASM.org

# Host and Bacterial Phenotype Variation in Adhesion of *Streptococcus mutans* to Matched Human Hosts

**Anders Esberg, Anna Löfgren-Burström, Ulla Öhman, and Nicklas Strömberg**

Department of Odontology/Cariology, Umeå University, Umeå, Sweden

**The commensal pathogen *Streptococcus mutans* uses AgI/II adhesins to adhere to gp340 adsorbed on teeth. Here we analyzed isolates of *S. mutans* ($n = 70$ isolates) from caries and caries-free human extremes ($n = 19$ subjects) by multilocus sequence typing (MLST), AgI/II full-length gene sequencing, and adhesion to parotid saliva matched from the strain donors (nested from a case-control sample of defined gp340 and acidic proline-rich protein [PRP] profiles). The concatenated MLST as well as AgI/II gene sequences showed unique sequence types between, and identical types within, the subjects. The matched adhesion levels ranged widely (40% adhesion range), from low to moderate to high, between subjects but were similar within subjects (or sequence types). In contrast, the adhesion avidity of the strains was narrow, normally distributed for high, moderate, or low adhesion reference saliva or pure gp340 regardless of the sequence type. The adhesion of *S. mutans* Ingbritt and matched isolates and saliva samples correlated ($r = 0.929$), suggesting that the host specify about four-fifths ($r^2 = 0.86$) of the variation in matched adhesion. Half of the variation in *S. mutans* Ingbritt adhesion to saliva from the caries cases-controls ($n = 218$) was explained by the primary gp340 receptor and PRP coreceptor composition. The isolates also varied, although less so, in adhesion to standardized saliva (18% adhesion range) and clustered into three major AgI/II groups (groups A, $B_1$, and $B_2$) due to two variable V-region segments and diverse AgI/II sequence types due to a set of single-amino-acid substitutions. Isolates with AgI/II type A versus types $B_1$ and $B_2$ tended to differ in gp340 binding avidity and qualitative adhesion profiles for saliva gp340 phenotypes. In conclusion, the host saliva phenotype plays a more prominent role in *S. mutans* adhesion than anticipated previously.**

*Streptococcus mutans* is considered a commensal pathogen for dental caries (30), a chronic infectious disease affecting billions of people worldwide (36). The cariogenic nature of *S. mutans* is related to its abilities to produce and withstand an acidic environment (9, 30), to form sticky biofilms (22, 30), and to attach to the saliva film on teeth (15, 20, 39). Accordingly, the underlying molecular traits, e.g., enolase, glycosyltransferases (GTFs), and AgI/II (SpaP or Pac) adhesins, have all been targets of vaccine and therapeutic strategies (10, 21, 24, 35).

*S. mutans* colonizes human subjects at low levels and prevalences. Multilocus sequence typing (MLST) shows a genetically homogenous but diverse *S. mutans* organism (4, 11, 33). Indeed, 122 sequence types (STs) out of 135 isolates occurred in caries cases and referents worldwide (11), and 92 sequence types occurred among 102 isolates from diverse human donors and origins (33). However, similar to other commensal pathogens, e.g., *Helicobacter pylori* (25), single genotypes of clones of *S. mutans* colonize and infect an individual host. Vertical mother-to-child transmission at infancy and horizontal transmission in the nursery accordingly involve only a few sequence types at the subject level (12, 26). However, although a high level of strain variation in adhesion (Adh) has been noted for a few laboratory and clinical isolates (6–8, 31), the strain variation in adhesion among clinical isolates from a homogenous sample and their relation to sequence types remain to be determined.

The AgI/II (SpaP or Pac) polypeptide is the primary adhesin on *S. mutans* for surface adhesion or solution aggregation by saliva (6, 18, 31). In contrast, commensal oral streptococci (e.g., *Streptococcus gordonii* and *S. sanguinis*) express AgI/II polypeptides among multiple other surface adhesins (19, 31). Moreover, AgI/II homologs are present in the invasive pathogens *S. pyogenes* and *S. agalactiae* (32). The AgI/II polypeptides are 140- to 180-kDa multidomain proteins with a structure composed of alanine-rich A, variable V, proline-rich P, and C-terminal C domains (27, 28). The V domain, which distinguishes the AgI/II SpaP and Pac variants in *S. mutans*, is considered more diverse than the A, P, and C domains (5, 19). Besides adhesion and aggregation (6, 18, 31), the AgI/II polypeptides mediate bacterial coaggregation (23) and modulate biofilm formation (1). AgI/II adopts an elongated fibrillar structure with the tip AVP and base $C_{12}$ domains both participating in saliva/gp340 binding (27, 28). However, little is known about the strain variation of AgI/II in modulating adhesion and host innate or immune defenses.

Saliva gp340 (or agglutinin/DMBT1) is the primary receptor for adhesion or aggregation by *S. mutans* and its AgI/II adhesin (13, 34). Saliva gp340 is an oligomeric mucin hybrid glycoprotein with multiple scavenger cysteine-rich domains with affinity for host ligands (e.g., collectins, secretory IgA, and lactoferrin) and O-glycosylated repeats with microbial binding sites (3, 17, 34). The saliva adhesion activity of *S. mutans* is modulated by gp340 size variants I to III and by allelic variants of acidic proline-rich protein (PRP) coreceptors (20, 39). Both the gp340 variant I and PRP Db polymorphisms coincide with *S. mutans* adhesion and caries experience (20, 39), and a low-avidity binding of *S. mutans* to PRPs has been reported (15). Moreover, in-depth studies on

Received 5 May 2012 Returned for modification 30 May 2012
Accepted 13 August 2012
Published ahead of print 27 August 2012
Editor: B. A. McCormick
Address correspondence to Nicklas Strömberg, nicklas.stromberg@odont.umu.se.

doi:10.1128/IAI.00435-12
The authors have paid a fee to allow immediate free access to this article.

low-, moderate-, and high-avidity saliva adhesion phenotypes of *S. mutans* indicated that the amount of gp340, PRP types, and inhibiting substances are adhesion modulatory (7). However, little is known about the relative roles of saliva and bacterial adhesion phenotypic variation, and their potential covariation, when human hosts and isolates of the commensal pathogen *S. mutans* are matched at a clinically significant level.

The aim of the present study was to explore the relative role and nature of saliva and bacterial adhesion phenotypes in the variation of *S. mutans* adhesion at a clinically significant level. We therefore analyzed a set of isolates of *S. mutans* ($n = 70$ isolates) from human caries ($n = 6$) or caries-free ($n = 13$) extremes by adhesion to parotid saliva matched from the same donors (nested from a larger sample of 12-year-old Swedish caries cases-controls; $n = 218$). The host types were resolved by gp340 and PRP profiling, and the bacterial types were resolved by MLST and AgI/II full-gene sequencing.

## MATERIALS AND METHODS

**Human parotid saliva samples and *S. mutans* isolates used.** The study was performed with the following biobank human and bacterial samples collected from two caries case-control cohorts of 12-year-old children in Västerbotten, Sweden ($n = 218$ [cohort 1] and $n = 246$ [cohort 2]): (i) isolates of *S. mutans* strains ($n = 70$ isolates) and parotid saliva samples matched from colonization-positive extremes of caries cases ($n = 6$ subjects; mean DeFSdefs [decayed into dentine, enamel caries included and filled, surfaces on permanent, DefS, and primary, defs, teeth] of 11 ± 3.5 standard deviations [SD]) and caries-free subjects ($n = 13$ subjects; mean DeFSdefs of 0 ± 0 SD), where isolates from caries-free donors (median of 3 isolates/donor) were obtained from buccal surfaces of teeth 34 to 36 and, in the case of donors with tooth decay, from different caries lesions (3 to 9 isolates/donor); (ii) parotid saliva from all caries cases and controls ($n = 218$) or parts selected thereof ($n = 81$) from the 218-subject cohort; and (iii) isolates of *S. mutans* ($n = 70$ isolates) sampled from 35 caries cases and 35 caries-free subjects from both cohorts ($n = 218$ and $n = 246$).

The study also used the following reference saliva samples from adult saliva donors: (i) reference parotid saliva samples, each with low-, moderate-, and high-avidity adhesion by *S. mutans* Ingbritt and (ii) reference parotid saliva samples, each with gp340 variant I, II, and III saliva phenotypes.

The study was approved by the Ethics Committee for Human Experiments at Umeå University, Sweden, and informed consent was given by the children and their parents. All parents signed consent to participate.

**Parotid saliva collection.** Parotid saliva was collected from the caries cases-controls by a trained dentist at the clinics using citric acid stimulation and Lashley cups.

***S. mutans* isolates and reference strains.** Plaque was sampled either from the buccal surfaces of teeth 34 to 36 of caries-free subjects or from caries lesions of subjects with tooth decay by using the following procedure. The plaque was sampled by using a foam pellet or a curette into 500 μl standard viability buffer (pH 7.2) and cultured on mitis-salivarius-bacitracin (MSB) plates. Four single isolates were then selected based on morphology and cultured on blood agar plates at 5% $CO_2$ in an aerobic environment for 2 to 3 days. Three isolates were recultured on blood agar plates and tested negative for arginase and positive for β-glucosidase activity and were then harvested and frozen in glycerol at −80°C.

*S. mutans* strain Ingbritt was from our stock collection, and *Lactococcus lactis* MG1363 expressing SpaP was kindly provided by H. Jenkinson, Bristol University.

**Culturing of bacteria and DNA isolation.** For DNA extraction or adhesion experiments, *S. mutans* strains were grown in Jordan broth at 37°C for 16 h. *Lactococcus lactis* MG1363 cells expressing SpaP were grown in M17 medium containing erythromycin (5 μg/ml) at 30°C for 16 h (18).

DNA was extracted from isolates of *S. mutans* as described previously (16). Briefly, DNA was released by enzymes, extracted by phenol-chloroform partitioning, and checked for purity (260/280 nm).

**MLST sequencing.** Gene segments were selected from the housekeeping genes *ppaC* (inorganic pyrophosphate), *pfl* (pyruvate formate lyase), *pyk* (pyruvate kinase), and *tuf* (elongation factor Tu) and from the *spaP* (surface AgI/II adhesin) gene and used for species typing and clonal resolution (4, 11). The gene segments were amplified from pure DNA by PCR using Kapa2G Robust Hotstart DNA polymerase (Kapa Biosystem) and the following primers: *pfl*-f (5′-ACGTTGCTTACTCTAAACAAACTGG-3′) and *pfl*-r (5′-ACTTCRTGGAAGACACGTTGWGTC-3′), *ppaC*-f (5′-GACCAYAATGAATTYCARCAATC-3′) and *ppaC*-r (5′-TGAGGNACMACTTGTTTSTTACG-3′), *pyk*-f (5′GCGGTWGAAWTCCGTGGTG-3′) and *pyk*-r (5′GCAAGWGCTGGGAAAGGAAT-3′), *tuf*-f (5′GTTGAAATGGAAATCCGTGACC-3′) and *tuf*-r (5′GTTGAAGAATGGAGTGTGACG-3′), and *spaP*-f (5′AGTGCGAGTAAGGAAG-3′) and *spaP*-r (5′TTCACCGCTGCCAAAT-3′). Amplified gene segments were purified and sequenced by MWG (Eurofins MWG Operon). All amplified gene segments were sequenced by using the amplification primers described above, except for *spaP*, where *spaP-seq*-f (TGCTAAGTCTGCTGGTGTCA) and *spaP-seq*-r [GCT(CT)GATAGTCTGCTTCG] were used. Forward and reverse sequences were aligned and trimmed by using the CodonCode Aligner program. Neighboring-joining trees were generated and sequence characteristics were determined by using MEGA5 and DnaSP software (29, 41). One strain failed repeatedly to return pure sequences. The MSLT sequences were submitted to the NIH NCBI genetic sequence database.

**Sequencing of the full-length AgI/II gene.** The full-length AgI/II gene was amplified from DNA purified from *S. mutans* isolates by PCR using Iproof DNA polymerase (Bio-Rad) and primers Ag-f (5′-GTTGGATAAAGTGTGGAGTTTGTG-3′) and Ag-r (5′-GCTCAATCTGTGATTTATCGCTTC-3′). Amplified AgI/II genes were purified and sequenced by Eurofins MWG Operon by using, in addition to Ag-f and Ag-r, the following sequencing primers: Ag-S1 (5′-GTTGGATAAAGTGTGGAGTTTGTG-3′), Ag-S2 (5′-CAGAAATTGCCGCTGCCAAT-3′), Ag-S3 (5′-CTTAAGGCTTCTGCTGTGGA-3′), Ag-S4 (5′-CAGTAGCTTCTCTTAACCG-3′), Ag-S5 (5′-GGCACCAGTAGCTCCAAAT-3′), Ag-S6 (5′-AGTTCCAGCTGAAGACAGCA-3′), Ag-S7 (5′-CGCTCTTCAGCAGATACCAT-3′), Ag-S8 (5′-GTTGATGGTCAGACTATTCC-3′), Ag-S9 (5′-TAGCAACTTCTGCCTCATGA-3′), Ag-S10 (5′-GGTTCTGTTAAGTTTCCGTC-3′), Ag-S11 (5′-CGGTTAAGAGAAGCTACTG-3′), Ag-S12 (5′-TGCTGTCTTCAGCTGGAACT-3′), Ag-S13 (5′-GGTTTACCAGGAGTTGTCAC-3′), Ag-S14 (5′-GGAATAGTCTGACCATCAAC-3′), Ag-S15 (5′-GCTCAATCTGTGATTTATCGCTTC-3′), Ag-S16 (5′-TGCTAAGTCTGCTGGTGTCA-3′), Ag-S17 (5′-GCTGATAGTCTGCTTCG-3′), Ag-S18 (5′-AAGCAAAACTTGCTAA-3′), Ag-S19 (5′-TCCTTTTCATAATTTG-3′), and Ag-S20 (5′-GAATTCTGCAGGTTAGTGTATGTA-3′). The generated gene segments were trimmed and assembled, covering both the forward and reverse strands of the full-length AgI/II gene, by using the CodonCode Aligner program. Neighboring-joining trees were generated and AgI/II characteristics were determined by using MEGA5 and DnaSP software (29, 41). The full-length AgI/II gene sequences were submitted to the NCBI GenBank database (see nucleotide sequence accession numbers below).

**Typing of AgI/II V-region types A and B among independent isolates.** Multiple independent isolates of *S. mutans* ($n = 70$) were typed as AgI/II V region type A or B by PCR amplification of the AgI/II gene as described above, followed by sequencing using primers Ag-S4 (5′-CAGTAGCTTCTCTTAACCG-3′) and Ag-S19 (5′-TCCTTTTCATAATTTG-3′).

**Bacterial adhesion.** The adhesion of metabolically $^{35}S$-labeled bacteria to saliva-coated hydroxyapatite beads (Bio-Rad Laboratories) was measured in 96-microtiter-well plates, as described previously (20, 31). Individual experimental runs were performed with all 70 isolates. After the hydration of the hydroxyapatite beads in adhesion buffer at 4°C overnight (5 mg beads in 125 μl per well), the beads were coated with 125 μl

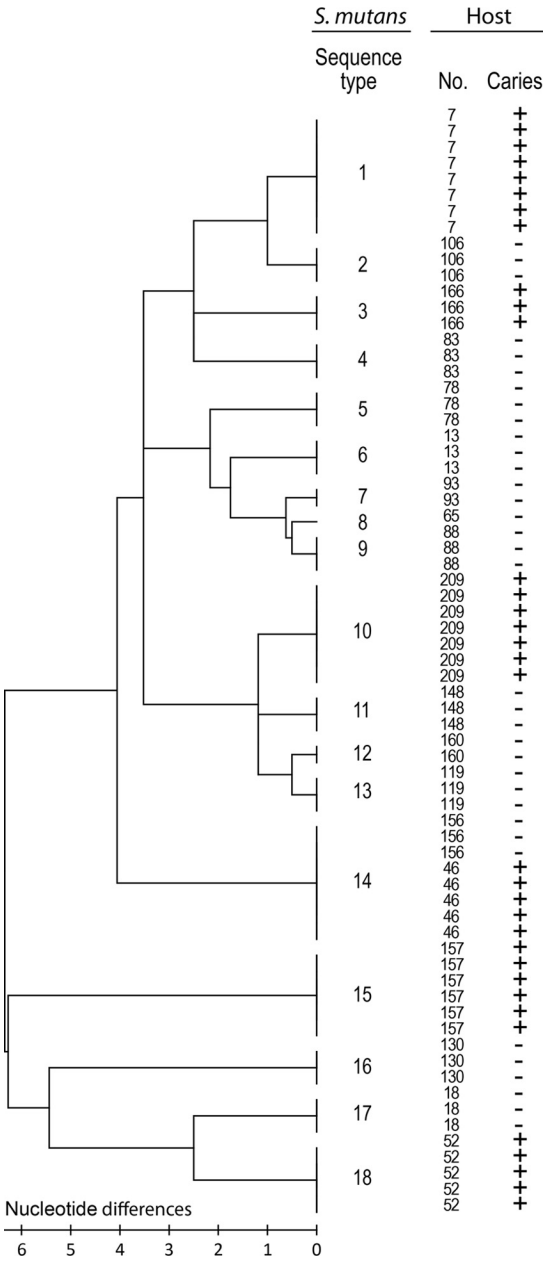


**FIG 1** Neighbor-joining tree showing diverse *S. mutans* sequence types (STs 1 to 18) between, while showing similar types within, caries (+) or caries-free (−) strain donors. The neighbor-joining tree was constructed from concatenated sequences of the housekeeping genes *pfl*, *pyk*, *tuf*, and *ppaC* and the AgI/II adhesin gene. The bar indicates the number of base differences per sequence.

saliva diluted 1:1 or 1:3 (matched samples) or with purified gp340 (6 μg/ml) for 1 h and washed. $^{35}$S-labeled bacteria were added (125 μl; $5 \times 10^8$ cells/ml; 1,000 cells/cpm) and incubated under agitation for 1 h. After unbound bacteria were washed away, the beads were counted with a scintillation counter, and the proportion of bound bacteria out of the total amount of added bacteria (percent adhesion) was calculated.

**AgI/II electrophoresis and Western blot analyses.** AgI/II proteins were localized and identified in bacterial outer surface protein extracts, essentially as described previously (18). Outer surface proteins were prepared from $5 \times 10^8$ bacterial cells according to standard methods. The resultant protein extract (15 μl), standardized by volume, was applied onto a 5% Criterion gel (Bio-Rad), separated, and silver stained according to the manufacturer's instructions (Thermoscientific) or subjected to Western blot analysis using AgI/II-specific antisera, a polyvinylidene difluoride (PVDF) membrane (Millipore), and 5% dried milk blocking solution. Densitometric values (intensity [INT] × mm$^2$) of the silver-stained AgI/II protein bands, as measured by the Chemidoc system (Bio-Rad), were used for the adjustment of adhesion relative to the amount/expression of AgI/II and the percent adhesion value/relative INT × mm$^2$ value.

**Slot blot measurements of gp340.** gp340 (or agglutinin) in parotid saliva was quantified in a slot blot overlay assay with monoclonal anti-gp340 antibody MAb-143 (1:60,000; kindly provided by D. Malamud, NYUCD), essentially as described previously (39). Briefly, saliva (diluted 1:50) was transferred onto a 0.45-μm nitrocellulose membrane (Protran BA85-SB; Whatman), followed by blocking with 5% dried milk in buffer (50 mM Tris, 150 mM NaCl [pH 7.4]) with 0.05% Tween 20, and incubated with MAb-143 for 1 h. After two washes, secondary antibody SAB-100 (1:60,000; Nordic Biosite AB, Sweden), a Super Signal West Dura detection kit (Pierce Protein Research Products), and densitometry (INT × mm$^2$) using the Chemidoc system (Bio-Rad) were used to quantify salivary gp340.

**Typing of phenotypes and allelic types of acidic PRPs.** Acidic PRPs in parotid saliva were typed on 7.0% (wt/wt) polyacrylamide (27:1 bis, wt/wt) gels by using a Protean IIxi apparatus (Bio-Rad) and quantified by densitometry (optical density [OD] per mm$^2$), as described previously (2). The samples were typed double blind; the vast majority were typed after a single run, and a few were typed after retyping with larger amounts. The allelic types (in parentheses) defined the following PRP phenotypes: P1 (PRP1/PIF), P4 (Db-PRP1/PIF), P5 (PRP2-PRP1/PIF), P6 (Pa-PRP2-PRP1/PIF), P7 (Db-Pa-PRP2-PRP1/PIF), P8 (Db-PRP2-PRP1/PIF), and P10 (Pa-PRP2).

**PLS modeling.** Partial least-squares (PLS) modeling, which relates two data matrices, *X* and *Y*, to each other by a linear multivariate prediction model (14, 42), was performed by using Simca+ P 12.01 (Umetrics AB, Umeå, Sweden). PLS modeling handles few or many, noisy, colinear, and incomplete *x* and *y* variables and data sets with *x* and *y* variables exceeding the observations (or subjects). The PLS model gives the ability of the *x* variables to explain ($R^2$) and, via cross-validation, to predict (a $Q^2$ value of <10% reflects a weak model) the variation in *Y*, variable characteristics (e.g., values for variable importance in the projection [VIP] of >1.0 mark influential *x* variables), and graphic plots (e.g., *x* and *Y* association structure). The data were log transformed and autoscaled to unit variance before being modeled.

**TABLE 1** Characteristics of loci and concatenated sequences of *S. mutans* isolates

| Locus[a] | No. of sequences | Fragment size (bp) | No. (%) of variable sites | G+C content | No. of allele types | No. of silent changes | No. of nonsilent changes | *k* | π |
|---|---|---|---|---|---|---|---|---|---|
| *tuf* | 69 | 405 | 4 (0.99) | 0.407 | 3 | 4 | 0 | 1.679 | 0.00414 |
| *ppaC* | 69 | 528 | 6 (1.14) | 0.372 | 6 | 4 | 2 | 1.960 | 0.00371 |
| *pyk* | 69 | 429 | 12 (2.80) | 0.394 | 9 | 11 | 1 | 3.014 | 0.00702 |
| *pfl* | 69 | 306 | 3 (0.98) | 0.392 | 3 | 3 | 0 | 0.226 | 0.00074 |
| *spaP* | 69 | 510 | 10 (1.96) | 0.396 | 9 | 8 | 2 | 1.899 | 0.00372 |
| Conc. | 69 | 2,178 | 35 (1.61) | 0.392 | 18 | 30 | 5 | 8.777 | 0.00403 |
| AgI/II | 69 | 4,704 | 259 (5.51) | 0.333 | 18 | 152 | 106 | 70.357 | 0.01503 |

[a] Conc. indicates concatenated sequences of *tuf*, *ppaC*, *pyk*, *pfl*, and *spaP* (*spaP* marks an AgI/II conserved segment). AgI/II indicates the full AgI/II gene sequence.

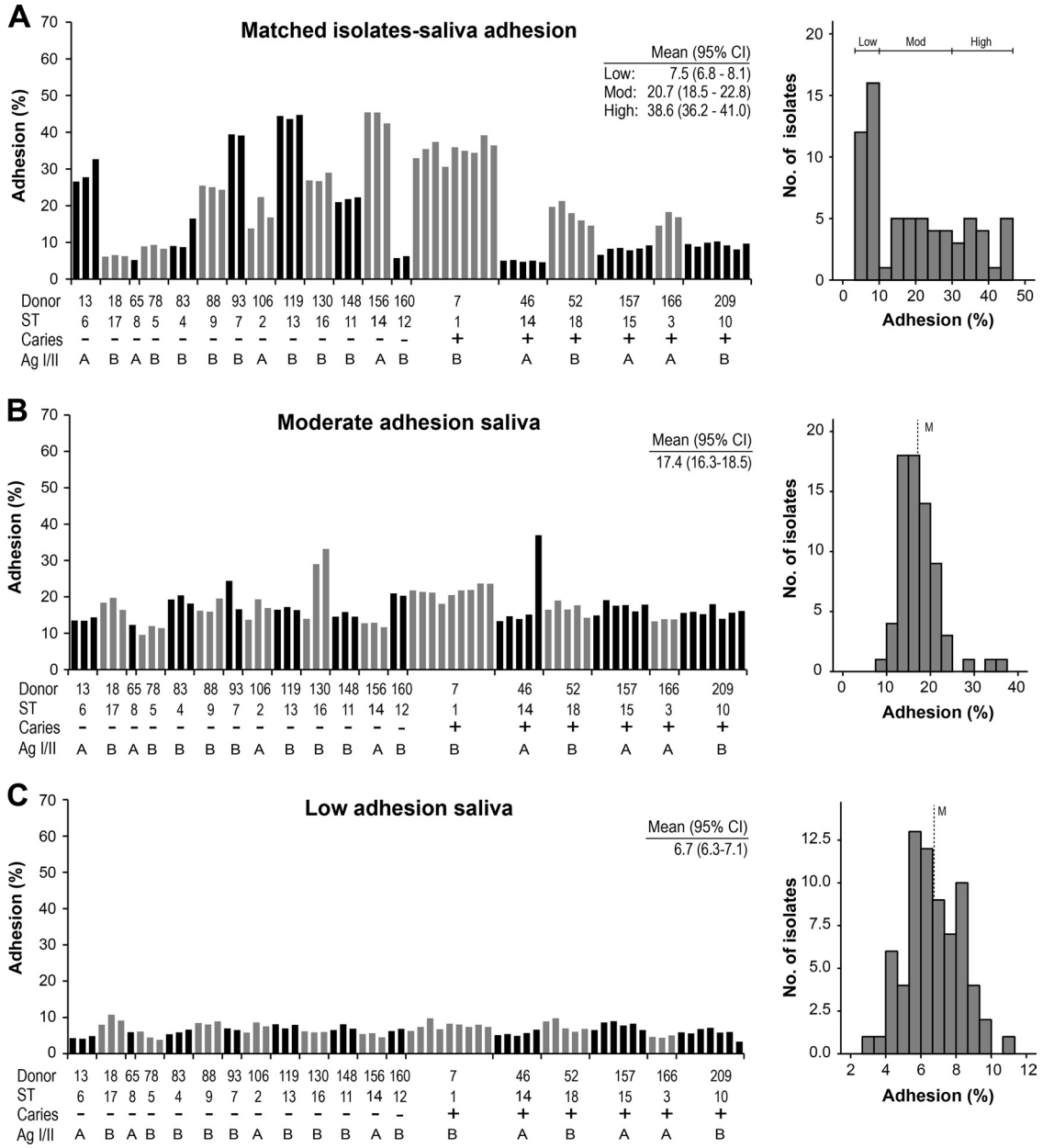


**FIG 2** Adhesion of *S. mutans* isolates ($n = 70$) to saliva matched from the strain donors and to moderate- and low-adhesion saliva. (A) Adhesion of *S. mutans* isolates ($n = 70$, each represented by a bar) or sequence types (STs) to saliva matched from caries (+) or caries-free (−) strain donors ($n = 19$). Adhesion (%) indicates the percentage of adhering cells of the total number of cells added. The histogram gives the distribution of adhesion among the isolates and defines the low-, moderate-, and high-adhesion phenotypes (right). Mean adhesion values (95% CI) for the low-, moderate-, and high-adhesion phenotypes are given. (B and C) Adhesion of *S. mutans* isolates to moderate-adhesion (B) and low-adhesion (C) saliva, together with histograms of the distribution of adhesion among isolates (right). Mean adhesion values (95% CI) are given. M, median adhesion.

The following qualitative and quantitative PRP and gp340 variables were modeled as *x* predictors: PRP phenotypes (Pp1 or P1 and Pp4 or P4, etc., P5, P6, P7, P8, and P10), total PRP amounts (PRPtot), allelic qualitative ($Db^+$, $Pa^+$, and $PRP1^+$ = PRP1/PIF-$s^+$, $PRP2^+$, and Db-$f^+$; $PRP3^+$ = PRP3/PIF-$f^+$), quantitative (Db, Pa, PRP1, PRP2, Db-f, and PRP3) types of PRPs, and total amounts of gp340. The *Y* variable was saliva adhesion of *S. mutans* Ingbritt.

**Traditional statistics.** Data are reported as means ± SD or means with 95% confidence intervals (CIs). We used a *t* test on log-transformed data for significant differences in means between adhesion groups and Pearson's or Spearman's test to correlate adhesion data. We used the Mann-Whitney U test for significant differences in medians between adhesion groups of isolates with AgI/II type A or B. We used SPSS software and considered differences significant at a *P* value of $<0.05$.

**Nucleotide sequence accession numbers.** The full-length AgI/II gene sequences were submitted to the NCBI GenBank database under accession numbers JX645983 to JX646051.

## RESULTS

**Unique sequence types of *S. mutans* within human subjects.** As a first step in exploring the adhesion of *S. mutans* isolates to

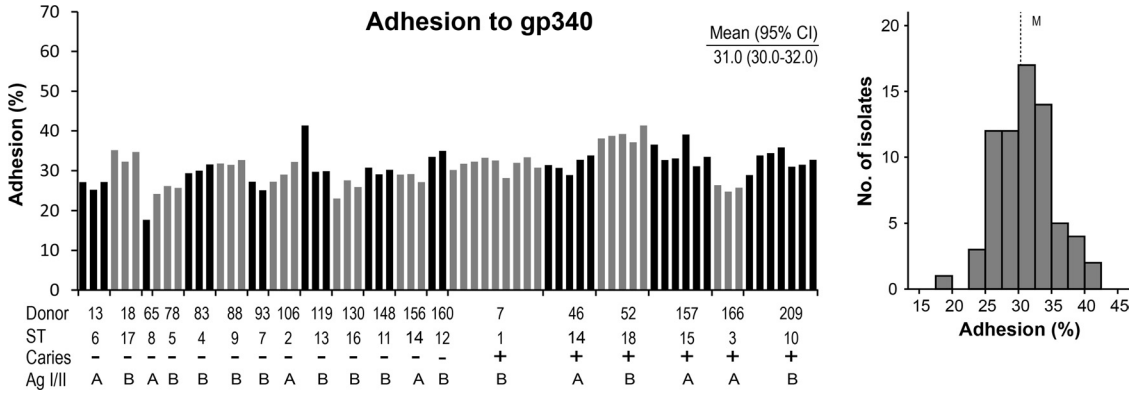


**FIG 3** Adhesion of *S. mutans* isolates ($n = 70$) or sequence types (STs) to pure gp340 receptor related to the caries (+) or caries-free (−) strain donors. Adhesion (%) indicates the percentage of adhering cells of the total number of cells added. The histogram (right) gives the distribution of adhesion among the isolates. Mean adhesion values (95% CI) are given. M, median adhesion.

matched saliva from donors, we measured the heterogeneity or genotypes of multiple isolates ($n = 70$) from high-caries ($n = 6$ subjects) or caries-free ($n = 13$ subjects) extremes (median, 3 isolates/subject). The isolates were genotyped by MLST sequencing of the conserved segments of the housekeeping genes *pyk*, *ppaC*, *tuf*, and *pfl* and the AgI/I adhesin gene previously used for species typing and the clonal resolution of viridians group streptococci (Fig. 1 and Table 1). The neighboring-joining tree of the concatenated sequences showed the same unique sequence types (STs) among isolates from the same subject. Accordingly, unique sequence types occurred between subjects (STs 1 to 13 and 15 to 18), except for the sharing of the same sequence type in two subjects (ST14). The housekeeping and the AgI/II adhesin genes had a low level of nucleotide diversity, and the sequence types thus differed by a few nonsilent amino acid substitutions (Table 1). Thus, each human subject appeared to be colonized by a unique sequence or "clonal" type regardless of the caries phenotype.

**The host phenotype is the major determinant for variation in matched isolate-saliva adhesion by *S. mutans*.** We measured the adhesion of the *S. mutans* isolates ($n = 70$) to parotid saliva samples matched from the strain donors and to reference saliva samples with a moderate or a low level of adhesion of *S. mutans* Ingbritt (Fig. 2). The matched adhesion (Adh) profile ranged widely (40% Adh range) and uniformly between subjects or sequence types, with low-avidity (<10% Adh; $n = 8$ subjects), moderate-avidity (10 to 30% Adh; $n = 7$), and high-avidity (>30% Adh; $n = 4$) adhesion phenotypes. In contrast, the matched adhesion profiles were similar within subjects and sequence types, except for ST14, which was shared by two subjects; all ST14 isolates from one subject (subject 156) had high levels of adhesion, and all isolates from the other subject (subject 46) had low levels of adhesion.

In contrast, the profiles of adhesion of the isolates to the moderate- or low-adhesion reference saliva samples were narrow, normally distributed, and of moderate or low avidity, respectively, regardless of the sequence type (Fig. 2B and C). Similarly, the profile of adhesion to the pure gp340 receptor protein was narrow, normally distributed, and of high avidity regardless of the sequence type (Fig. 3). Moreover, the adhesion of the isolates ($n = 70$) in two independent experiments (experiments 1 and 2) showed the same wide percent adhesion range for matched saliva-bacterium partners (40 and 45%) and a more narrow adhesion range for the unmatched low-adhesion (5 and 8%) and moderate-adhesion (14 and 15%) saliva samples or pure gp340 (15 and 24%) (Fig. 4A).

All sequence types of *S. mutans* (from all subjects) bound avidly to moderate-adhesion saliva, while they bound weakly to low-adhesion saliva (Fig. 4B). Moreover, high- and low-adhesion saliva samples were tested for the adhesion of *S. mutans* Ingbritt and three unique *S. mutans* sequence types (Fig. 4C). All strains bound avidly to the high-adhesion saliva and pure gp340 and weakly to the low-adhesion saliva. The relative strain adhesion capacity ranged from 25% to 44% and was the same regardless of the substrate used (Fig. 4C).

***S. mutans* Ingbritt mimics the adhesion of matched isolates-saliva samples.** In order to verify a predominant role of the host phenotype in matched saliva-bacterium adhesion, we compared the matched adhesion of the isolates with the adhesion of *S. mutans* model strain Ingbritt to the same saliva donors (Fig. 5). The *S. mutans* Ingbritt and matched adhesion profiles were highly correlated ($r = 0.929$; $P < 0.01$), verifying the representative nature of *S. mutans* Ingbritt and the somewhat homogenous adhesion behavior of the sequence types. Accordingly, up to four-fifths ($r^2 = 0.86$) of the variation in saliva adhesion may be attributable to the host phenotype. Moreover, *L. lactis* recombinantly expressing the AgI/II (SpaP) adhesin from *S. mutans* showed an adhesion profile highly reminiscent of that of strain Ingbritt ($r = 0.86$; $P < 0.01$) (Fig. 5), verifying that AgI/II is the predominant adhesin specifying the variation in *S. mutans* adhesion.

In addition, while the relative adhesion of the sequence types to the moderate- and low-adhesion saliva samples was correlated ($r = 0.61$; $P < 0.0061$) (Fig. 4B), the relative strain adhesion capacity did not correlate with the adhesion capacity of the matched isolates-saliva samples ($r = -0.14$; $P = 0.58$).

**Salivary gp340 receptors and PRP coreceptors partly explain the different host adhesion phenotypes.** Having shown that the adhesion of *S. mutans* Ingbritt is representative for the matched saliva-bacterium partners, we investigated the role of gp340 and PRPs in specifying the host adhesion phenotype. Multivariate PLS modeling (and traditional group statistics) were used to analyze the influence of the amount of saliva gp340 and the composition of acidic PRP on the saliva adhesion of *S. mutans* Ingbritt in two samples of subjects: a caries-referent sample of Swedish children

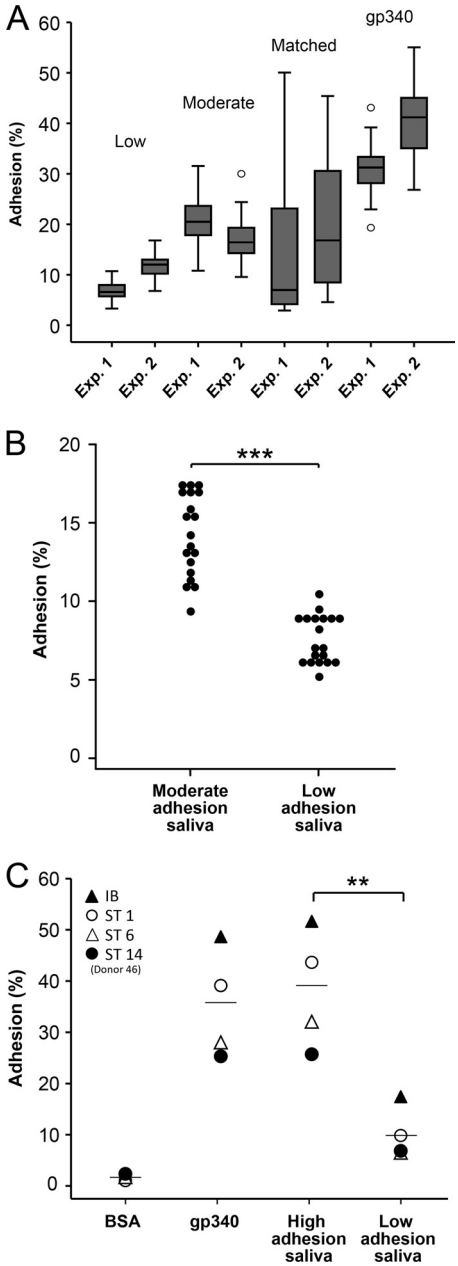


**FIG 4** (A) Adhesion of isolates ($n = 70$) in two independent experiments (Exp. 1 and Exp. 2) showing the same wide adhesion range for matched saliva-bacterium partners (45 and 40%) and a more narrow adhesion range for unmatched low-avidity (5 and 8%) and moderate-avidity (14 and 15%) saliva adhesion phenotypes or pure gp340 (15 and 24%). Adhesion (%) indicates the percentage of adhering cells of the total number of cells added. (B) Adhesion of all subject-specific sequence types ($n = 19$) to moderate- and low-adhesion saliva. Adhesion (%) indicates the percentage of adhering cells of the total number of cells added. ***, $P < 0.001$ by $t$ test. (C) Adhesion of *S. mutans* Ingbritt and sequence types 1, 6, and 14 (donor 46) to high- and low-adhesion reference saliva, pure gp340 receptor, and a bovine serum albumin (BSA) control. Adhesion (%) indicates the percentage of adhering cells of the total number of cells added. **, $P = 0.003$ by $t$ test.

($n = 218$) and low- and high-adhesion extreme samples selected thereof ($n = 81$) (Fig. 6 and Table 2).

The amount of gp340 and the acidic PRP composition explained and predicted half of the variation in adhesion ($n = 218$, $R^2 = 54\%$, and $Q^2 = 51\%$, and $n = 81$, $R^2 = 54\%$, and $Q^2 = 51\%$, respectively). The amount of gp340 was highly influential and correlated positively with adhesion (56.8% versus 18.2% mean adhesion for low versus high gp340 levels). The allelic types and phenotypes of PRPs were less influential, but their influence relative to that of gp340 increased for the adhesion extremes ($n = 81$; VIPs, 1:3) versus unselected adhesion phenotypes ($n = 218$; VIPs, 1:4). The P4 (PRP1 and Db) phenotype and allelic Db variant coincided positively (48.1% and 42.0% mean adhesions for P4 and Db subjects, respectively) with *S. mutans* adhesion in both models. In contrast, the P6 (Pa, PRP2, and PRP1) and P8 (Db, PRP2, and PRP1) phenotypes (31.6% and 9.2% mean adhesions for P6 and P8, respectively) and allelic PRP-2 and Pa variants coincided negatively.

**Unique AgI/II adhesin sequence and potential V-region binding types.** We further investigated the genetic heterogeneity of the AgI/II adhesin between and within subjects by sequencing the entire AgI/II adhesin gene from all isolates (Fig. 7 and Table 1). The neighboring-joining tree from a 5.5% nucleotide diversity (Table 1) displayed a unique AgI/II adhesin sequence type between most subjects (18 out of 19 subjects), while only two subjects shared AgI/II adhesin sequence types (Fig. 7A). All isolates from the same subject belonged to the same AgI/II adhesin sequence type.

The major AgI/II cluster groups A, $B_1$, and $B_2$ were derived from two variable V-region segments; one segment clustered all isolates into AgI/II type A or B, and the other (unique to the single AgI/II sequence type 18) clustered the isolates into AgI/II subtype $B_1$ or $B_2$ (Fig. 7A and B and 8C). A further set of single-amino-acid substitutions over the entire molecule specified the AgI/II adhesin sequence types.

Isolates with AgI/II type A ($n = 32$) tended to bind gp340 more avidly than did B-type strains ($n = 38$), particularly when adjusted for the amounts of AgI/II (Fig. 7C and 8D). We then measured V-region and gp340 binding avidity with a further set of independent isolates ($n = 70$), which showed significantly different gp340 binding for AgI/II type B versus type A isolates even when not adjusted for the amount of AgI/II, with median percent adhesions of 33.8 and 27.8%, respectively ($P = 0.016$ by Mann-Whitney U test) (Fig. 7C). Thus, AgI/II sequence variations may play modulatory roles in adhesion and gp340 binding.

In addition, the gel chromatograms of AgI/II showed a tendency toward a slightly shifted position of AgI/II type A (slower-migrating) versus type $B_1$ (faster-migrating) protein bands (Fig. 8D).

**Different adhesion profiles of *S. mutans* AgI/II adhesin types for saliva gp340 phenotypes I to III.** We next analyzed a representative isolate of each cluster group and AgI/II types A, $B_1$, and $B_2$ for adhesion to various amounts of gp340 and to saliva gp340 phenotypes I to III, each characterized by a specific gp340 size variant, variant I, II, or III (Fig. 8). The isolates displayed gp340 avidity binding in the order of AgI/II type $B_1$ (isolate no. 7) > type $B_2$ (isolate no. 166) > type A (isolate no. 78) upon repeated dose-response experiments. While the AgI/II B-type isolates with moderate to high gp340 adhesion (isolates no. 7 and 166) displayed adhesion profiles similar to the saliva phenotypes I to III (II > I and III), the AgI/II A-type isolate with low gp340 binding (isolate no. 78) bound saliva avidly but with another profile (III > II > I). The AgI/II type A, $B_1$, and $B_2$ isolates (no. 78, 7, and 166, respectively) appeared to express similar amounts of AgI/II (Fig. 8D), further supporting strain differences in gp340 and saliva adhesion among the AgI/II adhesin types.

## DISCUSSION

This study reveals findingsof host and bacterial phenotypic variation in host saliva-*S. mutans* adhesion matched at a clinically sig-

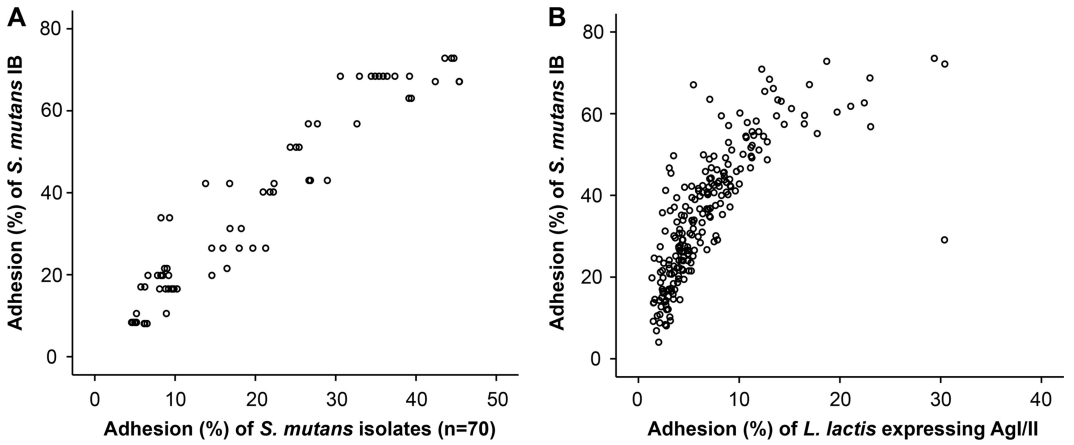


**FIG 5** (A) Scattergram of the adhesion of *S. mutans* Ingbritt (IB) (*y* axis) and of the isolates ($n = 70$) (*x* axis) to parotid saliva from strains donors ($n = 19$) ($r = 0.929$). Adhesion (%) indicates the percentage of adhering cells of the total number of cells added. (B) Scattergram of the adhesion of *S. mutans* Ingbritt (*y* axis) and of *L. lactis* MG1363 recombinantly expressing AgI/II (*x* axis) to saliva samples from multiple subjects ($n = 218$) ($r = 0.86$).

nificant level. Although both the host and bacterial phenotypes modify adhesion, the host phenotype played a strikingly large role in specifying a low, moderate, or high level of adhesion of matched *S. mutans* isolates-saliva samples. Several findings allowed this conclusion: (i) a wide (low to moderate to high) adhesion profile occurred for *S. mutans* isolates and saliva samples matched from the same donor, as opposed to the narrow, normally distributed adhesion profile when the same isolates were attached to a refer-

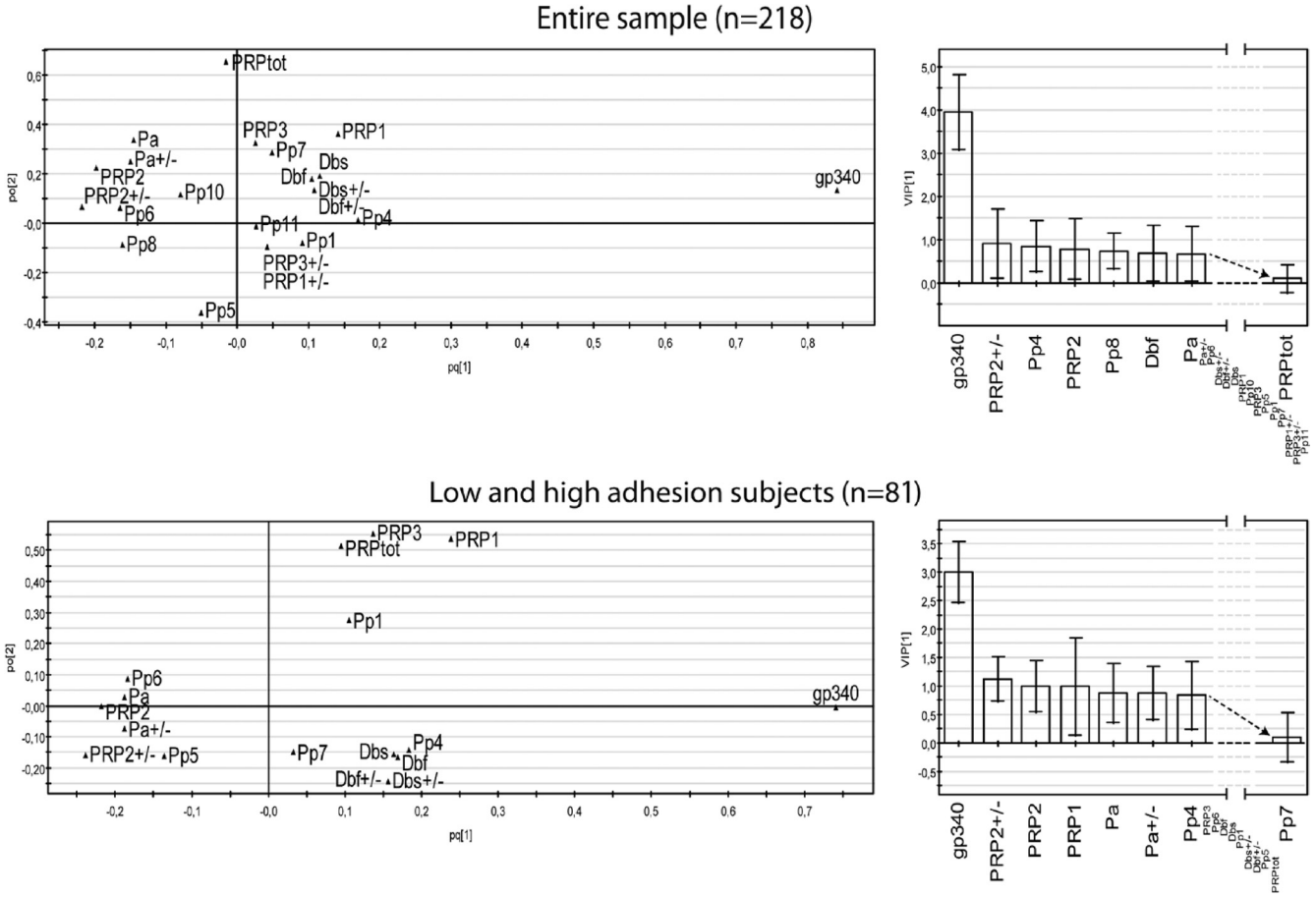


**FIG 6** Partial least-squares (PLS) plots of the structure of the association between the amount of gp340; PRP allelic types (e.g., Db and PRP2), phenotypes (e.g., Pp4), and amounts (PRPtot); and the adhesion of *S. mutans* Ingbritt to saliva from donors from a caries case-referent sample ($n = 218$) or from high- or low-adhesion saliva extremes selected thereof ($n = 81$) (bottom). The variable importance in the projection (VIP) is given for selected variables (right). pc[1], correlated variation; po[2], noncorrelated variation (noise).

**TABLE 2** *S. mutans* adhesion by PRP coreceptors and gp340 primary receptor phenotypes

| Phenotype | Composition | All subjects ($n = 218$) | | | Adhesion extremes ($n = 81$) | | |
|---|---|---|---|---|---|---|---|
| | | Prevalence (%) (no. of subjects) | Mean % adhesion of *S. mutans* | 95% CI | Prevalence (%) (no. of subjects) | Mean % adhesion of *S. mutans* | 95% CI |
| P4 | Db, PRP1/PIF | 18 (40) | 40.2 | 35.3–45.2 | 17 (14) | 48.1 | 35.4–60.8 |
| P6 | Pa, PRP2, PRP1/PIF | 28 (62) | 32.8 | 28.7–37.0 | 30 (24) | 31.6 | 21.4–41.8 |
| P8 | Db, PRP2, PRP1/PIF | 4 (8) | 25.8 | 15.6–36.0 | 2 (2) | 9.2 | 4.5–22.7 |
| $PRP2^+$ | | 47 (103) | 33.0 | 30.0–36.1 | 48 (39) | 30.4 | 23.0–37.9 |
| $Db^+$ | | 31 (67) | 38.0 | 34.1–41.9 | 28 (23) | 42.0 | 31.6–52.4 |
| High gp340 | > median | 50 | 45.1 | 42.6–47.6 | 50 | 56.8 | 52.6–61.0 |
| Low gp340 | < median | 50 | 26.1 | 23.7–28.5 | 50 | 18.2 | 13.8–22.8 |

ence saliva sample; (ii) the host phenotype accordingly mediated a low, moderate, or high level of adhesion irrespective of MLST, the AgI/II sequence type, or the host origin of the isolates; and (iii) the profiles of adhesion of the matched isolates-saliva samples and of *S. mutans* Ingbritt to the same saliva samples were highly correlated ($r = 0.929$), verifying a largely similar adhesion behavior of the *S. mutans* isolates or sequence types and the representative nature of *S. mutans* Ingbritt as a model bacterium. We thus ex-

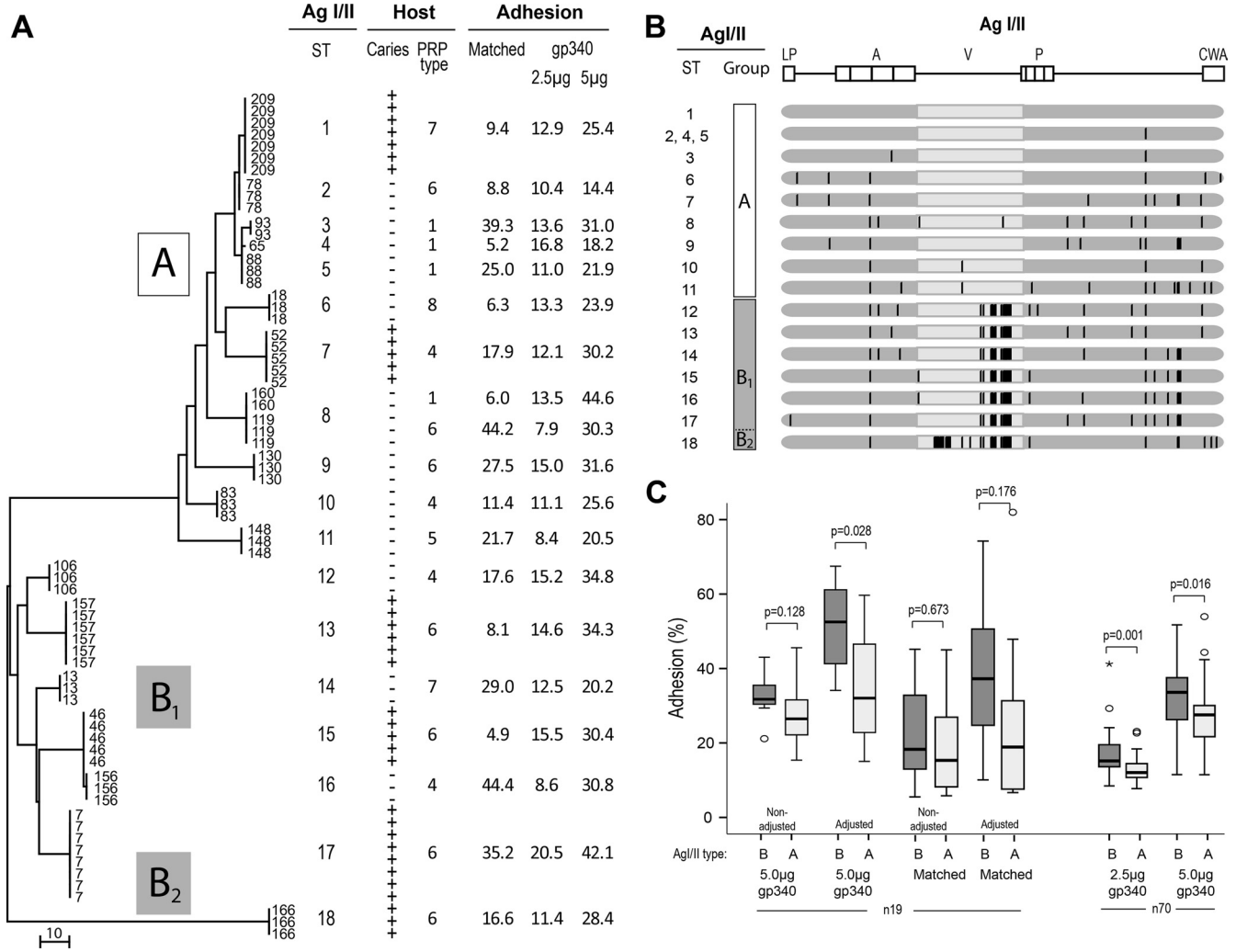


**FIG 7** AgI/II adhesin sequence types. (A) Neighboring-joining tree from the AgI/II full-gene sequences showing a diversity of AgI/II adhesin sequence types (AgI/II STs 1 to 18) between human hosts ($n = 19$ subjects) of defined caries, PRP, and adhesion phenotypes. The bars indicate the number of base differences per sequence. (B) Schematic picture of the AgI/II amino acid variations and substitutions related to each AgI/II adhesin sequence type (a solid vertical line marks each amino acid substitution). The leader peptide (LP), alanine-rich repeats (A), variable domain (V), proline-rich domain (P), and cell wall anchorage (CWA) region are marked. (C) Relative avidity of adhesion of independent isolates ($n = 19$ or $n = 70$) with AgI/II type A or B to gp340 (2.5 and 5.0 μg) or matched saliva, unadjusted or adjusted for the expression level of AgI/II. Adhesion (%) indicates the percentage of adhering cells out of the total cells added. *P* values derived by a Mann-Whitney test are given.

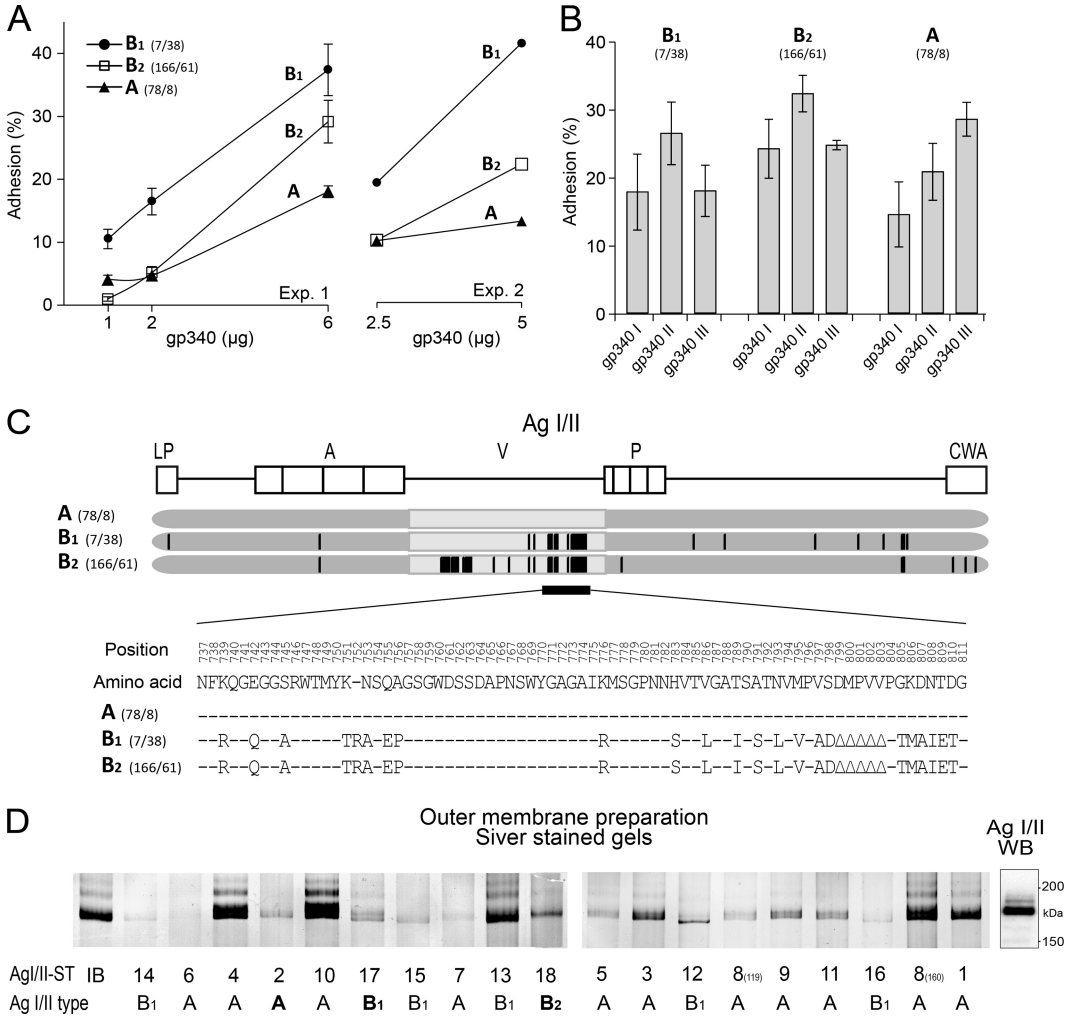


**FIG 8** *S. mutans* AgI/II types with different profiles of adhesion to saliva gp340 phenotypes I to III. (A) Adhesion of *S. mutans* AgI/II types to various amounts of gp340 in two separate experimental runs. Adhesion (%) indicates the percentage of adhering cells of the total number of cells added. (B) Adhesion of the *S. mutans* AgI/II types to saliva phenotypes with gp340 size variants I, II, and III. Adhesion (%) indicates the percentage of adhering cells of the total number of cells added. Shown are mean adhesion values and 95% CIs. (C) Schematic illustration of the structural variations of the AgI/II types. (D) AgI/II protein pattern for the independent isolates ($n = 19$) shown by silver staining of outer membrane surface extracts after electrophoresis on 5% gels. The AgI/II sequence types (STs 1 to 18) and AgI/II types A, $B_1$, and $B_2$ are marked. A Western blot (WB) with anti-AgI/II antibodies marks the reported position of the AgI/II protein band (18).

trapolate that about four-fifths ($r^2 = 0.86$) of the variation in saliva adhesion should be attributed to the host phenotype and that about one-fifth (14%) should be attributed to the bacterial phenotype. Thus, both host and strain phenotypic variation should be considered in persistent infectious diseases.

Together, the primary gp340 receptors and PRP coreceptors explained half of the variation in *S. mutans* Ingbritt adhesion between the human subjects. While the amount of the primary gp340 receptor (present in all subjects) played a clearly dominant role, the PRP phenotypes (present at various frequencies) apparently also modified the saliva adhesion behavior, e.g., mean percent adhesions of 48.1% (95% CI, 35.4 to 60.8%) for P4 and 9.2% (95% CI, 4.5 to 22.7%) for P8. Indeed, the influence of PRPs relative to that of gp340 increased for adhesion extremes ($n = 81$ subjects) versus all subjects ($n = 218$ subjects), indicating that largely different receptor/coreceptor "haplotypes" may be at work at the subject level. Notably, the quality (but not quantity) of PRPs modified adhesion, as opposed to gp340. Accordingly, gp340 size variants I to III, which are known to modify adhesion and caries susceptibility, could explain a further portion of the variation in *S. mutans* Ingbritt adhesion. Moreover, the P4 (PRP1 and Db) phenotype and the allelic Db variant promoted, while P6 (Pa, PRP2, and PRP1) and PRP2 diminished, *S. mutans* adhesion. Accordingly, both allelic and "haplotype" variations modify *S. mutans* adhesion. The PRP coreceptors (although devoid of avid *S. mutans* binding) and specific phenotypes may mediate the low-avidity binding of *S. mutans* or indirectly affect the adsorption, presentation, or intermolecular behavior of the gp340 receptor in the saliva film. We do not know whether the high-avidity saliva adhesion phenotype reflects a misbehaving saliva gp340 aggregation function in a subset of human subjects.

The findings or conclusions of the present study are facilitated by the identical "clonal" and AgI/II sequence types within, but unique sequence types between, human subjects. Indeed, the concatenated sequences of conserved gene loci (MLST) and AgI/II adhesin full-length gene sequences revealed 18 unique sequence

types among 19 host subjects, while isolates from the same subject (and different caries lesions) shared the same sequence type. We thus confirm data from previous reports of *S. mutans* as a genetically homogenous but diverse organism and the presence of a few sequence types or genotypes in individual subjects. In the present homogenous, although limited, *S. mutans* sample (from defined plaque sites of Swedish 12-year-old subjects), however, both the AgI/II nucleotide diversity (1.96% versus 7.99%) and the frequency of single sequence types appeared to be lower than reported previously. The either poor or good saliva adhesion phenotypes of the *S. mutans* colonization-positive children studied here, regardless of the sequence type, does not simply argue for matched saliva-isolate adhesion as a primary selection mechanism for the different clonal types between subjects. Host immunological surveillance and tolerance, and other as-yet-unknown and diverse mechanisms, may account for this selection of clonal types. Regardless, we suggest that there is a diverse *S. mutans* population and that a single or a few sequence types or "clones" adhere, colonize, and persist at the subject level regardless of a healthy or decayed condition.

The AgI/II adhesin types derived from two variable V-region segments that grouped AgI/II into type A or types $B_1$ and $B_2$ ($B_{1,2}$) and single-amino-acid substitutions (single-nucleotide polymorphisms [SNPs]) over the entire molecule. We hypothesize that these sequence variations contribute to quantitative and qualitative differences in saliva adhesion and gp340 binding among the isolates, partly because multiple independent isolates of AgI/II type A or B differed significantly in their gp340 binding avidities and partly because a strain each of AgI/II types A and $B_{1,2}$ had qualitatively different profiles of adhesion to saliva gp340 phenotypes I to III. Notably, the V region is localized at the AgI/II binding tip, and adhesin sequence variations, including single-amino-acid substitutions, are known to modulate epitope specificity related to different host niches and tropisms (37, 38, 40, 43). Nevertheless, the overall homogenous AgI/II structure agrees both with the representative nature of the model adhesion strain Ingbritt and with the overall low level of strain variation in adhesion relative to the host phenotype. Whether AgI/II sequence variation is related to particular saliva adhesion subtypes (e.g., gp340/PRP phenotypes) or other host innate or immune defenses related to infection susceptibility remains to be determined.

Dental caries and *S. mutans* represent a prominent model to study infection susceptibility and the behavior of commensal pathogens in persistent infections. Here we used a few independent *S. mutans* isolates and human subjects ($n = 19$) from a larger clinical or biobank sample of caries and caries-free subjects to highlight the importance of the host phenotype in the matched adhesion of saliva-*S. mutans* partners and, thus, potentially in caries susceptibility (20, 39). We also used the biobank sample of independent human subjects ($n = 81$ and $n = 218$) or isolates ($n = 70$) to further explore the host receptor and bacterial adhesin phenotypes. However, further studies using larger samples of human cases and isolates will be required to explore the host and bacterial phenotypes in infection susceptibility and cariogenicity, respectively, and their possible coevolution. Nevertheless, such studies will ultimately guide the selection of reference and type strains for in-depth basic molecular biology and translational research studies.

## ACKNOWLEDGMENTS

The study was financially supported by the Swedish Medical Research Council (grant 10906); the Faculty of Odontology, Umeå University; and the Västerbottens County Council.

## REFERENCES

1. **Ahn SJ, Ahn S-J, Wen ZT, Brady LJ, Burne RA.** 2008. Characteristics of biofilm formation by *Streptococcus mutans* in the presence of saliva. Infect. Immun. **76**:4259–4268.
2. **Azen EA, Yu PL.** 1984. Genetic polymorphisms of Pe and Po salivary proteins with probable linkage of their genes to the salivary protein gene complex (SPC). Biochem. Genet. **22**:1065–1080.
3. **Bikker FJ, et al.** 2004. Bacteria binding by DMBT1/SAG/gp-340 is confined to the VEVLXXXXW motif in its scavenger receptor cysteine-rich domains. J. Biol. Chem. **279**:47699–47703.
4. **Bishop CJ, et al.** 2009. Assigning strains to bacterial species via the Internet. BMC Biol. **7**:3. doi:10.1186/1741-7007-7-3.
5. **Brady LJ, et al.** 1991. Restriction fragment length polymorphisms and sequence variation within the *spaP* gene of *Streptococcus mutans* serotype c isolates. Infect. Immun. **59**:1803–1810.
6. **Brady LJ, Piacentini DA, Crowley PJ, Oyston PCF, Bleiweis AS.** 1992. Differentiation of salivary agglutinin-mediated adherence and aggregation of mutans streptococci by use of monoclonal antibodies against the major surface adhesin P1. Infect. Immun. **60**:1008–1017.
7. **Carlén A, Bratt P, Stenudd C, Olsson J, Strömberg N.** 1998. Agglutinin and acidic proline-rich protein receptor patterns may modulate bacterial adherence and colonization on tooth surfaces. J. Dent. Res. **77**:81–90.
8. **Carlén A, Olsson J, Börjesson AC.** 1996. Saliva-mediated binding *in vitro* and prevalence *in vivo* of *Streptococcus mutans*. Arch. Oral Biol. **41**:35–39.
9. **de Soet JJ, Nyvad B, Kilian M.** 2000. Strain-related acid production by oral streptococci. Caries Res. **34**:486–490.
10. **Dinis M, et al.** 2011. rEnolase maternal immunization confers caries protection on offspring. J. Dent. Res. **90**:325–330.
11. **Do T, et al.** 2010. Generation of diversity in *Streptococcus mutans* genes demonstrated by MLST. PLoS One **5**:e9073. doi:10.1371/journal.pone.0009073.
12. **Doméjean S, et al.** 2010. Horizontal transmission of mutans streptococci in children. J. Dent. Res. **89**:51–55.
13. **Ericson T, Rundegren J.** 1983. Characterization of a salivary agglutinin reacting with a serotype c strain of *Streptococcus mutans*. Eur. J. Biochem. **133**:255–261.
14. **Eriksson L, et al.** 2004. Using chemometrics for navigating in the large data sets of genomics, proteomics, and metabonomics (gpm). Anal. Bioanal. Chem. **380**:419–429.
15. **Gibbons RJ.** 1989. Bacterial adhesion to oral tissues: a model for infectious diseases. J. Dent. Res. **68**:750–760.
16. **Hallberg K, Holm C, Öhman U, Strömberg N.** 1998. *Actinomyces naeslundii* displays variant fimP and fimA fimbrial subunit genes corresponding to different types of acidic proline-rich protein and beta-linked galactosamine binding specificity. Infect. Immun. **66**:4403–4410.
17. **Holmskov U, et al.** 1999. Cloning of gp-340, a putative opsonin receptor for lung surfactant protein D. Proc. Natl. Acad. Sci. U. S. A. **96**:10794–10799.
18. **Jakubovics NS, Strömberg N, van Dolleweerd CJ, Kelly CG, Jenkinson HF.** 2005. Differential binding specificities of oral streptococcal antigen I/II family adhesins for human or bacterial ligands. Mol. Microbiol. **55**:1591–1605.
19. **Jenkinson HF, Demuth DR.** 1997. Structure, function and immunogenicity of streptococcal antigen I/II polypeptides. Mol. Microbiol. **23**:183–190.
20. **Jonasson A, et al.** 2007. Innate immunity glycoprotein gp-340 variants may modulate human susceptibility to dental caries. BMC Infect. Dis. **7**:57. doi:10.1186/1471-2334-7-57.
21. **Kelly CG, et al.** 1999. A synthetic peptide adhesion epitope as a novel antimicrobial agent. Nat. Biotechnol. **17**:42–47.
22. **Koga T, Asakawa H, Okahashi N, Hamada S.** 1986. Sucrose-dependent cell adherence and cariogenicity of serotype c *Streptococcus mutans*. J. Gen. Microbiol. **132**:2873–2883.
23. **Kolenbrander PE, et al.** 2002. Communication among oral bacteria. Microbiol. Mol. Biol. Rev. **66**:486–505.
24. **Krüger C, et al.** 2002. *In situ* delivery of passive immunity by lactobacilli producing single-chain antibodies. Nat. Biotechnol. **20**:702–706.

25. **Kusters JG, van Vliet AH, Kuipers EJ.** 2006. Pathogenesis of *Helicobacter pylori* infection. Clin. Microbiol. Rev. **19**:449–490.
26. **Lapirattanakul J, et al.** 2008. Demonstration of mother-to-child transmission of mutans streptococci using multilocus sequence typing. Caries Res. **42**:466–474.
27. **Larson MR, et al.** 2011. Crystal structure of the C-terminal region of *Streptococcus mutans* antigen I/II and characterization of salivary agglutinin adherence domains. J. Biol. Chem. **286**:21657–21666.
28. **Larson MR, et al.** 2010. Elongated fibrillar structure of a streptococcal adhesin assembled by the high-affinity association of alpha- and PPII-helices. Proc. Natl. Acad. Sci. U. S. A. **107**:5983–5988.
29. **Librado P, Rozas J.** 2009. DnaSP v5: a software for comprehensive analysis of DNA polymorphism data. Bioinformatics **25**:1451–1452.
30. **Loesche WJ.** 1986. Role of *Streptococcus mutans* in human dental decay. Microbiol. Rev. **50**:353–380.
31. **Loimaranta V, et al.** 2005. Fluid- or surface-phase human salivary scavenger protein gp340 exposes different bacterial recognition properties. Infect. Immun. **73**:2245–2252.
32. **Maddocks SE, et al.** 2011. *Streptococcus pyogenes* antigen I/II-family polypeptide AspA shows differential ligand-binding properties and mediates biofilm formation. Mol. Microbiol. **81**:1034–1049.
33. **Nakano K, et al.** 2007. *Streptococcus mutans* clonal variation revealed by multilocus sequence typing. J. Clin. Microbiol. **45**:2616–2625.
34. **Prakobphol A, et al.** 2000. Salivary agglutinin, which binds *Streptococcus mutans* and *Helicobacter pylori*, is the lung scavenger receptor cysteine-rich protein gp-340. J. Biol. Chem. **275**:39860–39866.
35. **Russell MW, Childers NK, Michalek SM, Smith DJ, Taubman MA.** 2004. A caries vaccine? The state of the science of immunization against dental caries. Caries Res. **38**:230–235.
36. **Selwitz RH, Ismail AI, Pitts NB.** 2007. Dental caries. Lancet **369**:51–59.
37. **Sharon N.** 2006. Carbohydrates as future anti-adhesion drugs for infectious diseases. Biochim. Biophys. Acta **1760**:527–537.
38. **Sokurenko EV, et al.** 1998. Pathogenic adaptation of *Escherichia coli* by natural variation of the FimH adhesin. Proc. Natl. Acad. Sci. U. S. A. **95**:8922–8926.
39. **Stenudd C, et al.** 2001. The association of bacterial adhesion with dental caries. J. Dent. Res. **80**:2005–2010.
40. **Strömberg N, et al.** 1990. Host-specificity of uropathogenic *Escherichia coli* depends on differences in binding specificity to Gal alpha 1-4Gal-containing isoreceptors. EMBO J. **9**:2001–2010.
41. **Tamura K, et al.** 2011. MEGA5: molecular evolutionary genetics analysis using maximum likelihood, evolutionary distance, and maximum parsimony methods. Mol. Biol. Evol. **28**:2731–2739.
42. **Trygg J, Wold S.** 2002. Orthogonal projections to latent structures (OPLS). J. Chemom. **16**:119–128.
43. **Xu R, McBride R, Paulson JC, Basler CF, Wilson IA.** 2010. Structure, receptor binding, and antigenicity of influenza virus hemagglutinins from the 1957 H2N2 pandemic. J. Virol. **84**:1715–1721.